Available online at www.sciencedirect.com
SCIENCE DIRECT
Polymer 46 (2005) 3957–3970
polymer
www.elsevier.com/locate/polymer

Feature Article

Methods to improve the properties of polymer mixtures: optimizing intermolecular interactions and compatibilization

E. Eastwood, S. Viswanathan, C.P. O'Brien, D. Kumar, M.D. Dadmun*

Chemistry Department, University of Tennessee, 321 Buehler Hall, Knoxville, TN 37996, USA

Received 16 November 2004; accepted 15 February 2005
Available online 9 April 2005

Abstract

Two methods to improve the dispersion, interfacial adhesion and properties of polymer mixtures are presented. Infrared spectroscopy and optical microscopy results document that control of the spacing of interacting moieties along the polymer chain results in optimal intermolecular hydrogen bonding and improved miscibility between two polymers. Moreover, initial results indicate that this protocol also works for polymer nanocomposites. Computational and experimental results indicate that multiblock or blocky copolymers are the most effective interfacial strengtheners among linear copolymers for polymer–polymer interfaces. ADCB and neutron reflectivity experiments provide direct evidence that multiblock copolymers that have blocks that are long enough to entangle with a homopolymer are most effective at strengthening the interface. Both sets of results provide guidelines by which multi-component polymer systems can be designed with target properties.

Keywords: Blends; Nanocomposites; Compatibilization

1. Introduction

Polymers offer a wide variety of properties that make them ideal materials for a broad range of applications, from polyethylene in garbage and sandwich bags to poly (*p*-phenylene terephthalamide) in bulletproof jackets. Moreover, there is a fairly solid understanding of the relationship between the molecular level structure of a polymer and its ultimate properties. For instance, it is well known that the low surface energy of the fluorine groups in Teflon provides the well-known 'nonstick' behavior of poly(tetrafluoroethylene).

However, the choice of a material for a new application in the real world is complex. The new application will come with a range of specific property requirements; the material must be so transparent, so impact resistant, so oxygen permeable, so flexible… Unfortunately, it is often difficult to pull a polymer off the shelf that will have all of the required material properties. One solution to this problem is to add a second component to the polymer to create a new material with targeted properties. Ideally, the original polymer will have many of the required properties, however, the addition of a second component (filler, plasticizer, second polymer) will create a new material with all of the required properties. For instance, in an ideal world, poly(ethylene) could be mixed in all proportions to poly(*p*-phenylene terephthalamide) to create a range of materials where its properties would vary linearly with composition from the flexibility and elasticity of garbage bags to the extraordinary strength of bulletproof jackets. Unfortunately, this systematic alteration of properties is not readily observed because most polymer pairs do not mix.

Flory–Huggins theory provides the framework to explain this mixing behavior. Flory–Huggins theory [1–3] is a mean-field, lattice model theory that provides an expression for the change in Gibbs free energy upon mixing two dissimilar polymers, polymers A and B

$$\frac{\Delta G_m}{RT} = \frac{\Phi_A}{M_A} \ln \Phi_A + \frac{\Phi_B}{M_B} \ln \Phi_B + \chi_{AB} \Phi_A \Phi_B \quad (1)$$

where Φ_A and Φ_B, and M_A and M_B are the volume fractions and degrees of polymerization of polymers A and B,

* Corresponding author. Tel.: +1 865 974 6582.
E-mail addresses: dad@utk.edu (M.D. Dadmun), dadmun@novell.chem.utk.edu (M.D. Dadmun).

0032-3861/$ - see front matter © 2005 Elsevier Ltd. All rights reserved.
doi:10.1016/j.polymer.2005.02.073

respectively, and χ_{AB} is the Flory interaction parameter. The first two terms on the right hand side of this equation denote the configurational entropy of mixing two long chain molecules, which quantitatively is negative, but very small as M_A and M_B are large numbers for polymers. Moreover, the value of χ_{AB} usually tends to be positive when accounting for dispersion forces between the mixed polymers. Thus, most polymer mixtures are immiscible, as a value of $\Delta G_m < 0$ denotes a process that will result in a miscible system and the combination of small negative entropy of mixing and a larger positive χ_{AB} means ΔG_m will usually be positive.

The result, on a molecular level is shown in Fig. 1, which illustrates the interface between two polymers that do not thermodynamically mix. This is an interface where there exist very few entanglements between the two polymers, resulting in a very weak system, and a macroscopic material whose properties fall far short of those targeted.

Thus, the lack of miscibility, and resultant weak interfaces between phase-separated domains, dramatically limit the ability to create new materials with targeted properties from polymer mixtures. Moreover, it is well understood that, in phase-separated mixtures, the dispersion of the minor phase in the surrounding matrix and the interfacial adhesion between the two phases are critical in creating a useful material [4]. If the minor phase can be homogeneously dispersed throughout the matrix and there exists good interfacial adhesion between the two phases, the properties of the phase-separated mixture can be dramatically improved and approach that of a miscible system. Moreover, a miscible system can be thought of as a system where the dispersion of the minor phase in the matrix has extended to the molecular level. Therefore, if a sample that is usually immiscible can be modified to create a miscible system, then this process can be thought of as optimally improving the 'dispersion' of the minor phase.

Thus, control of the dispersion and interfacial adhesion between phases of a multiphase polymer system is critical in order to create useful polymer mixtures. This article will present research results from our group that attack the problem of improving the properties of a phase-separated polymer mixture using two different methods and is meant to review the progress that our research group has made in this research area. The first method concentrates on improving the miscibility of a polymer blend by incorporating functional groups on one polymer to introduce intermolecular interactions (hydrogen bonding) between the two polymers. In this method, it is found that spacing the hydrogen bonding moieties on the polymer chain optimizes the extent of intermolecular interactions. The second method to improve phase-separated polymer mixtures determines the impact of copolymer microstructure on its ability to behave as a polymeric surfactant that can be added to a polymer blend to improve the dispersion and interfacial adhesion between two components in a phase separated polymer mixture. In this method, it is found that the sequence distribution of a linear copolymer dramatically influences its ability to modify polymer–polymer interfaces.

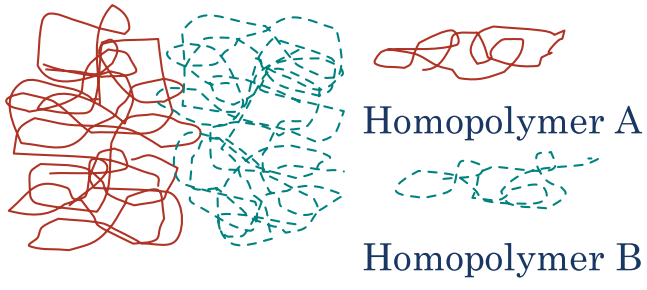

Fig. 1. Diagram of the interface between two immiscible polymers. The lack of entanglement between the two polymers at the interface results in a material with poor macroscopic properties.

2. Experimental

2.1. Materials and polymer synthesis

For the asymmetric double cantilever beam (ADCB) and neutron reflectivity experiments, Polystyrene (PS) was purchased from Aldrich with a M_w of 230,000 and a M_n of 140,000. Atactic poly(methyl methacrylate) (PMMA) was purchased from Polysciences, Inc. with a M_w equal to 100,000 and a M_n of 62,500. Both homopolymers were heated at 150 °C under vacuum for 48 h to remove any remaining solvent or other impurities. A poly(styrene$_{93.5\ K}$-b-methyl methacrylate$_{108\ K}$) diblock was purchased from Polymer Source, Inc., while a poly(styrene$_{0.7}$-ran-methyl methacrylate$_{0.3}$) random copolymer was synthesized via free radical techniques in our lab [5]. Multiblock copolymers were synthesized using ATRP (atom transfer radical polymerization) techniques as previously reported [6]. A difunctional initiator (phenoxybenzene-4,4′-disulfonyl chloride) was used in the presence of a copper halide/2,2′-bipyridine complex to sequentially polymerize alternating blocks of styrene and methyl methacrylate.

The liquid crystalline polyurethane (LCPU) used in the hydrogen bonding studies was synthesized by the condensation of 4,4′-bis(6-hydroxyhexoxy) biphenyl (BHHBP) and 2,4-toluene diisocyanate (TDI) according to literature procedures [7,8]. BHHBP was also prepared according to literature procedures via the condensation of 4,4-biphenol with 6-chlorohexanol. Poly(styrene-*co*-4-vinyl phenol) (PS-*co*-VPh) random copolymers for these studies were prepared by the free radical polymerization of styrene and 4-acetoxy styrene using AIBN as the initiator followed by the hydrolysis of the acetoxy groups using hydrazine hydrate according to the procedure of Green and Khatri [9]. Copolymers containing 5, 10, 20, 30, 40 and 50 mol% vinyl phenol were synthesized and utilized in this study. Hereinafter, PS-*co*-VPh(n) denotes a PS-*co*-VPh copolymer with *n* mol% VPh. The molecular weight characteristics and thermal behavior of these polymers are listed in Table 1.

Table 1
Molecular weight and thermal characteristics of copolymers of styrene and vinyl phenol

Polymer	Molecular weight (g/mol)		T_g
	M_n	M_w	
LCPU	35,000	53,600	87
PS-*co*-VPh(5)	13,700	21,300	101
PS-*co*-VPh(10)	20,700	34,500	103
PS-*co*-VPh(20)	47,100	90,100	105
PS-*co*-VPh(30)	22,100	32,400	108
PS-*co*-VPh(40)	31,300	61,100	114
PS-*co*-VPh(50)	34,100	65,200	116
PVPh	22,000	–	147

2.2. Experimental techniques

Molecular weights of the synthesized polymers were determined using a Waters Gel Permeation Chromatograph equipped with ultrastyragel columns with a refractive index detector. Differential scanning calorimetry (DSC) measurements were carried out to determine the thermal properties of the polymers and their blends and were run at 10 °C/min using a Mettler DSC 821 calibrated with Indium.

Composition of the copolymers used in the ADCB and reflectivity experiments was measured by proton NMR (^{1}H NMR). Degrees of polymerizations for the multiblocks' initial blocks were found by GPC. However, due to increasing polydispersity, the degrees of polymerization of the remaining blocks were obtained from the NMR composition data. It is important to note that, due to the sequential nature of this synthetic procedure, it is expected that the multiblock copolymers will exhibit narrow composition distributions, a parameter that is also known to be important in the interfacial modification process by copolymers [10,11].

For the asymmetric double cantilever beam experiments, polystyrene (PS) and poly(methyl methacrylate) (PMMA) homopolymers were compression molded and then cut into strips that were 1 cm wide, 6.5 cm long, and either 0.20 cm thick for the PMMA layer or 0.23 cm thick for the PS layer. This difference in thickness is required to help minimize craze formation and help maintain the crack propagating at the interface [12–14]. If both layers were the same thickness, the crack may swerve into the more compliant material, in this case, PS. This would cause the formation of crazes which would inflate the measured fracture toughness as energy would go into their formation rather than propagate along the crack; therefore, the PS was made slightly thicker than the PMMA layer. The thickness ratio used in this study ($h_{PS}/h_{PMMA} = 1.1$) was found by Winey [15], and later a similar value (1.2) was found by Brown [16], to be the optimal thickness ratio for a PS/PMMA system in ADCB experiments. Copolymer layers ranging from 20 to 300 nm were spin coated from a copolymer solution (toluene) onto a glass slide at 2500 rpm for 30 s. The thickness of the copolymer film was controlled by the concentration of the solution, which varied from 0.7 to 5.3 wt%. The copolymer films are floated off the glass slide into a water bath and floated onto the PS strip. The samples were dried at 80 °C for at least 2 h and then dried at the same temperature under vacuum for 24 h. A PMMA strip was placed on top of the copolymer layer resulting in a three-layer sandwich (PS/copolymer/PMMA). This tri-layer sample was annealed for 2 h at 150 °C under slight pressure. The final ADCB samples were then stored in a dessicator until testing by ADCB. This annealing time and temperature was used in order to be consistent with similar ADCB studies of styrene/methyl methacrylate copolymers given in the literature [10,12,15,16]. Also, increasing the annealing time from 2 to 18 h was reported by H.R. Brown to give little variation in fracture toughness [13].

The fracture toughness was measured by the asymmetric double cantilever beam (ADCB) test [13,17,18]. In short, a razor blade is driven into an interface, where a crack develops. The length of the crack from the razor blade edge to the crack tip, a, is measured and correlated to the fracture toughness of the interface by Eq. (2).

$$G_c = \frac{3\Delta^2 E_1 h_1^3 E_2 h_2^3 E_1 h_1^3}{8a^4} \frac{E_1 h_1^3 C_2^2 + E_2 h_2^3 C_1^2}{[E_1 h_1^3 C_2^3 + E_2 h_2^3 C_1^3]^2} \quad (2)$$

where $C_1 = 1 + 0.64\, h_1/a$ and $C_2 = 1 + 0.64\, h_2/a$

In Eq. (2), a is the crack length, Δ is the thickness of the razor blade, and h_1 and h_2 are the thickness of the homopolymer layers. E_1 and E_2 are Young's moduli of the homopolymers and were found by three point flexural test (ASTM D790). For each copolymer examined, 7–12 samples were tested.

For the hydrogen bonding studies, infrared spectroscopy data were obtained on a Biorad FTS-60A Fourier Transform Infrared (FT-IR) spectrometer purged with dried air using a minimum of 64 scans at a resolution of 2 cm^{-1}. The frequency scale was calibrated internally with a He–Ne reference to an accuracy of 0.2 cm^{-1} and externally with polystyrene. Samples for FT-IR studies were obtained by solvent casting blends of LCPU and PS-*co*-VPh from DMF (2% w/v) on KBr disks at room temperature. The KBr disks were placed on a horizontal holder in a dessicator to reduce the evaporation rate and to avoid film cracking. After evaporating most of the solvent at room temperature, the disks were subsequently dried in a vacuum oven at 60 °C for 3 days to remove residual solvent and moisture. The absence of solvent in the sample was verified by the absence of the C=O peak of DMF which occurs at 1650 cm^{-1} in the IR curve, which occurs at a lower wavenumber than the C=O peak of the LCPU (1730 cm^{-1}). The films prepared for FTIR were adequately thin to be within an absorbance range where the Beer–Lambert law is satisfied.

To determine the phase behavior of blends, a blend solution of 2% (w/v) in DMF was prepared and subsequently spotted on a microscope slide. This was dried in a dessicator first and then overnight in a vacuum oven at 60 °C. Using an Olympus BH-2 optical microscope

equipped with a Mettler FP82HT hot stage, phase behavior studies were completed by examining the temperature dependence of samples using phase contrast and polarized optical microscopy.

The samples for the neutron reflectivity (NR) experiments were constructed by spin coating a deuterated poly(methyl methacrylate) (dPMMA) film (56 nm) on a silicon wafer followed by floating a layer of the protonated copolymer (35 nm) on top of the dPMMA. Finally, a layer of deuterated polystyrene (dPS) (56 nm) was floated from a glass slide onto the copolymer to create a sandwich of copolymer between the dPS and dPMMA. The resulting sample was then annealed at 150 °C for 12 h. NR measurements for the trilayer samples were performed on the NG-1 reflectometer at the National Center for Neutron Research at the National Institute of Standards and Technology in Gaithersburg, MD. The wavelength of the neutrons used was 4.75 Å with a wavelength spread of 0.05 Å. The intensity of neutrons reflected from these multilayers was monitored and recorded as a function of angle incident on the sample. This reflected intensity was transformed into the reflectivity of the sample by subtracting background and normalizing to the intensity of the incident neutron beam and plotted as a function of q_z which $=4\pi/\lambda \sin(\theta)$ where λ is the wavelength of neutron and θ is the incident angle. The reduced data were then fit using the REFLFIT program provided by NIST to generate scattering length density profiles.

3. Results and discussion

3.1. Optimized intermolecular interactions

The concept that is examined in this set of experiments is to understand the options available to a scientist to optimize the extent of intermolecular hydrogen bonding between two polymers and correlate this extent of intermolecular hydrogen bonding to the phase behavior of the resultant blends, and is exemplified in Fig. 2. For instance, assume that one of the polymers in Fig. 1 contains a carbonyl or ether oxygen, a functional group that can accept a hydrogen bond. If the other polymer is now modified to contain a hydrogen bonding donating group, such as hydroxyl groups (Fig. 2A), the two molecules can now form a desirable enthalpic attraction between the two molecules, which may be conducive to forming a more miscible system. However, there exists a parameter that has been overlooked in this discussion that may be quite important, the amount of hydrogen bonding groups (hydroxyl) that exist on the modified second polymer. A simple argument can be made that this parameter will, in fact be quite important in optimizing the extent of intermolecular hydrogen bonds between the two polymers. As shown in Fig. 2B, the hydroxyl groups can easily be introduced into the polymer at any level by simply copolymerizing two monomers, one that contains the hydrogen bonding group and one that does not (i.e. styrene and vinyl phenol). Thus, 5%, 10%, 50% or 100% of the monomers on that chain may contain the hydroxyl group. The impact of the change in the amount of the hydroxyl group in the copolymer chain on the amount of intermolecular hydrogen bonds can be argued as follows. As hydroxyl groups are added to the polymer at low percentage hydroxyl, the addition of each hydroxyl group will result in more intermolecular hydrogen bonding between the hydroxyl and the hydrogen bonding accepting group on the other polymer and thus there is an increase in the plot in Fig. 2B at the low end of the x-axis. However, at the other end of the x-axis, where the polymer contains hydroxyl groups on nearly every monomer, there exists a significant amount of intramolecular hydrogen bonding (OH–OH hydrogen bonds) that limits the ability of a given hydroxyl group to find and orient correctly with a hydrogen bonding accepting group of the other polymer to form an intermolecular hydrogen bond. Thus by decreasing the number of hydroxyl groups in this regime, the amount of intramolecular hydrogen bonding should decrease, improving the probability that a given hydroxyl group can form an intermolecular hydrogen bond and there will exist a corresponding increase in the amount of intermolecular hydrogen bonding between the two polymers as the number of hydroxyl groups decreases from near 100%. Thus, there must exist some composition of the copolymer where the amount of intermolecular hydrogen bonding is optimum, as shown in the plot in Fig. 2B.

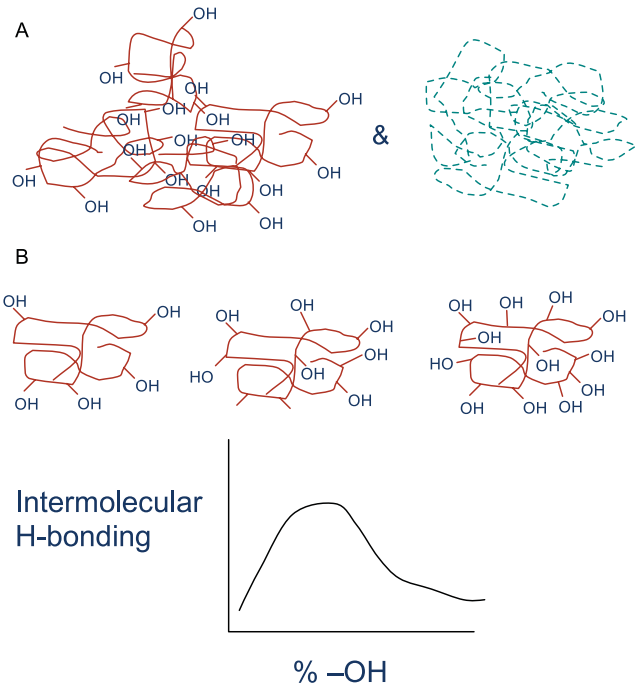

Fig. 2. Structures illustrating the incorporation of hydrogen bonding moieties in blend components to introduce intermolecular interactions. In this figure, it is assumed that the second polymer (dashed lines) contains a hydrogen bonding acceptor group, such as an ether oxygen or carbonyl group.

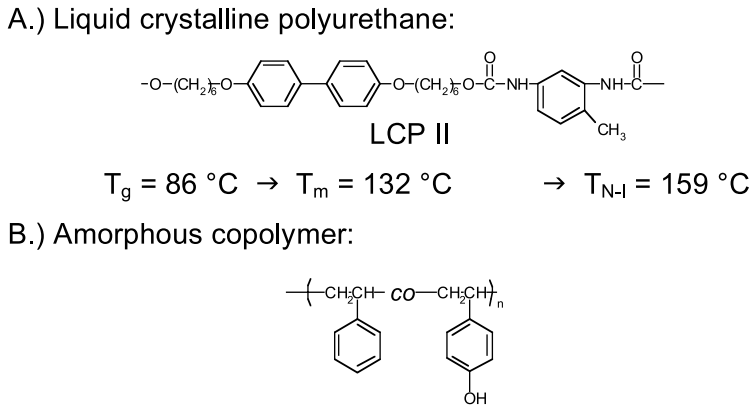

Fig. 3. Structures of the two components used in the optimization of intermolecular hydrogen bonding study.

This concept of improving miscibility by introducing and optimizing the extent of intermolecular interactions between two polymers has been applied in our lab to the blend of a liquid crystalline polymer and an amorphous polymer. The impetus for using a liquid crystalline polymer (LCP) in this study is two-fold. First, liquid crystalline polymers are intriguing materials that have been commercially available for over 30 years, but have not found widespread applications [19–21]. This lack of acceptance has been mostly driven by its high cost and difficulty in processing. Some of the same properties that give a liquid crystalline polymer its strength, i.e. backbone rigidity, also make it difficult to dissolve in common solvents [22]. Thus, if an LCP can be thermodynamically mixed with a less costly polymer, a molecular composite can be formed that would exploit the excellent properties of the LCP at a much lower cost. A second driving force to examine this concept with LCP as one of the components is that mixing a coil-like polymer and a rod-like polymer is more difficult than mixing two coil-like polymers. Flory first pointed out many years ago [23,24], that when rods and coils try to mix, the rods tend to phase separate into a separate phase to align, excluding the coils. Thus, if this concept of optimizing intermolecular hydrogen bonds between two components can create an increased miscibility window in blends of rods and coils, it should work for most other polymer blends as well.

The structure of the liquid crystalline polyurethane (LCPU) used in these studies is shown in Fig. 3, as well as the general structure of the amorphous copolymer, a copolymer of styrene and vinyl phenol, PS-*co*-VPh. As previously reported [8,25], the extent of intermolecular hydrogen bonding between the carbonyl of the LCPU and the hydroxyl of the styrenic copolymer is quantified by Fourier Transform Infrared Spectroscopy (FTIR) as a function of the composition of the copolymer for various blend compositions. These results are then interpreted to correlate the extent of intermolecular hydrogen bonds to the amount of hydroxyl functional groups present in the mixture. These results are shown in Fig. 4 where this figure is a plot of the percent of carboxyl groups that are hydrogen bonded to hydroxyl groups (i.e. intermolecular hydrogen bonds) as a function of the composition of the styrenic copolymer. Each curve is for a given blend composition, so going up the *x*-axis corresponds to increasing the amount of hydroxyl groups that are present in the blend. Examination of this curve shows that, at the low end of the curve, as the amount of hydroxyl groups increases, the amount of intermolecular hydrogen bonding increases. This makes sense; as more –OH groups are added into the blend, more of them find –COO– groups to form hydrogen bonds with and the number of intermolecular hydrogen bonds increases. However, once the blend contains a certain amount of hydroxyl groups, it appears that adding more –OH does not increase the amount of intermolecular hydrogen bonds, i.e. the curve levels off. This suggests that copolymers with more than 20% vinyl phenol in the copolymer do not benefit from the presence of more –OH. From this data, it appears that the optimum amount of intermolecular hydrogen bonding occurs for the PS-*co*-VPh copolymer that contains 20% vinyl phenol in this blend. Moreover, the goal of optimizing the extent of hydrogen bonding is to create a blend with better dispersion and/or broader miscibility window, thus determination of the phase diagram of the blends of the LCPU with the various copolymers is needed. These phase diagrams have been determined using optical microscopy and are shown in Fig. 5. Not surprisingly, this figure shows that there is an improvement in the miscibility of the blend as the amorphous polymer is changed from the PS-*co*-VPh that contains 10% –OH to the copolymer with 20% –OH, corresponding to an increase in the extent of intermolecular hydrogen bonds. As the amount of –OH is further increased to 30%, however, the miscibility decreases, corresponding to the IR results that showed very little change in the amount of intermolecular hydrogen bonding going from 20 to 30% vinyl phenol in the copolymer.

Thus, these results show that the largest miscibility

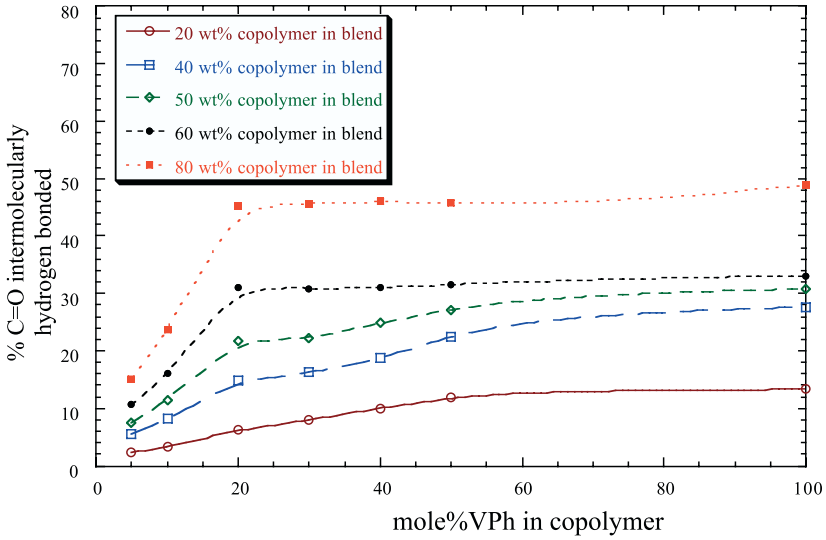

Fig. 4. FTIR results that quantify the amount of intermolecular hydrogen bonding to a carbonyl on the LCPU as a function of the copolymer composition.

window in these blends corresponds to the system that demonstrates the optimum amount of intermolecular hydrogen bonding, as measured by FTIR. However, why is 20% the optimum composition? The argument presented in the discussion of Fig. 2 is too simplistic to capture all of the physics that drive this optimization of intermolecular hydrogen bonding. Hydrogen bonds are interactions that require the two participating moieties to be in the proximity of each other and aligned correctly to form the intermolecular interaction. Thus, a given –OH group must have dynamic mobility to explore space, find a carbonyl, and orient itself correctly with respect to the carbonyl in order to form an intermolecular hydrogen bond. However, if a given –OH group is adjacent or in close proximity on a polymer chain to another –OH that participates in hydrogen bonding, that first –OH group will not have the dynamic mobility needed to successfully capture a carbonyl to form another intermolecular hydrogen bonding. It is only when the –OH groups are adequately spaced out along the chain that the hydrogen bonding moieties become sufficiently independent to form the optimum amount of intermolecular hydrogen bonds for a given blend. This concept of –OH group accessibility to form intermolecular hydrogen bonds has been quantified and verifies this physical explanation [25,26].

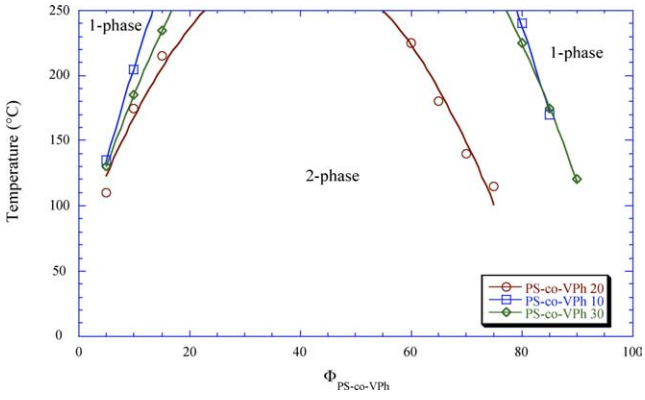

Fig. 5. Phase diagrams of LCPU-PS-*co*-VPh blends, documenting the impact of the styrenic copolymer composition on the miscibility of the blend.

Thus, separating the interacting moieties along the polymer chain provides a mechanism to optimize the amount of intermolecular interaction between two polymers, as this provides dynamic independence to the interacting functional groups that are bound to the polymer chain. Moreover, these results also indicate that miscibility may be induced between two polymers with only slight modification of the structure and properties of one polymer. For instance, if a miscible blend of polystyrene and this LCPU is the targeted mixture, modifying 20% of the polystyrene monomers to vinyl phenol provides a route to the desired product. Moreover, this modification is a modest change that only slightly alters the properties of the components, such as its glass transition and solubility.

3.1.1. Nanocomposites

Our group has also recently extended this concept to polymer nanocomposites. For instance, in polymer clay nanocomposites, it is possible to disperse a small amount of layered silicates in a polymer and dramatically alter its thermal and structural properties [27–29]. However, these property improvements are most effective when the 1 nm thick clay sheets are individually dispersed in the polymer matrix. Unfortunately, most polymers will not exfoliate the clay sheets, and thus this property improvement is not observed for many polymer–clay mixtures. More likely, the clays clump together in phase separated domains or are partially penetrated by the polymer to form an intercalated structure. Thus, it is desirable to provide a controllable

mechanism to create an exfoliated nanocomposite for a given polymer matrix.

There has been evidence presented that improved intermolecular interactions (such as hydrogen bonding) between a polymer and a clay will provide an impetus to form an exfoliated nanocomposite. This is best exemplified by the work of a number of workers to successfully produce a polyolefin/clay nanocomposite where the clay is exfoliated by the polymer melt [30–35]. The exfoliation of organomodified layered silicates (OLS) by a nonpolar polyolefin is assumed to be limited by the highly polar clay surfaces. These workers have found that polyolefin oligomers with polar functionality intercalate into the silicate galleries during melt blending, which in turn allowed the exfoliation of the silicates by polyolefins. More specifically, the melt blending of polypropylene with maleic anhydride modified polypropylene (MA-PP) in the presence of OLS resulted in a system where a large fraction of the silicates were exfoliated. The authors most often attributed this phenomena with 'strong hydrogen bonding between the maleic anhydride groups with the polar clay surfaces.' [28]. However, the authors offer no proof of the presence of hydrogen bonding between the MA-PP and the clay nor do they provide systematic evidence that the inclusion of functionalized oligomers may be a general method to improve the dispersion of an OLS in other (primarily nonpolar) polymers. Thus there is a need to systematically evaluate the role and ability of hydrogen bonding between an organophilic clay and a functionalized polymer to provide cohesive guidelines by which a broad range of polymers can be reinforced with exfoliated clay sheets on the nanoscale.

Thus, experiments that examine the influence of the extent of intermolecular hydrogen bonding on the dispersion of layered silicates in a polymer matrix is examined. Nanocomposites of Nanomer 1.24TL from Nanocor (Arlington Heights, IL) with polystyrene-*co*-vinyl phenol are examined at 5% clay loading, where the amount of vinyl phenol in the copolymer is varied from 0 to 100%. Nanomer 1.24TL is a clay that has 12-amino dodecanoic acid as a surfactant. A multi-step process that includes sonication of the clay and polymer in THF, continuous stirring of this dispersed solution, and precipitation, filtration, and drying of the sample produced the nanocomposites. The dispersion of these nanocomposites was then monitored using small angle X-ray scattering. These SAXS curves are shown in Fig. 6.

The SAXS pattern of the neat clay shows a clear peak at $q = 0.36$ Å^{-1}, which corresponds to a spacing of 17.4 Å between the clay sheets. Addition of this clay to polystyrene or a PS-*co*-VPh copolymer with 20% vinyl phenol show no noticeable change in the SAXS scattering indicating that the polymer is not penetrating into the clay galleries significantly. As the styrenic copolymer becomes more polar and the amount of vinyl phenol is increased to 30 and 40% the peak in the SAXS curve decreases dramatically, suggesting that these copolymers can penetrate into the galleries, create hydrogen bonds with the clay and exfoliate the clay. Note, however, that for both of these nanocomposites, a broad peak centered around $q = 0.36$ Å^{-1} does remain, indicating that the exfoliation is not complete. However, as the styrenic polymer becomes poly(vinyl phenol), the stronger peak reappears, albeit at a lower q value, indicating an intercalated structure. These results will be presented in

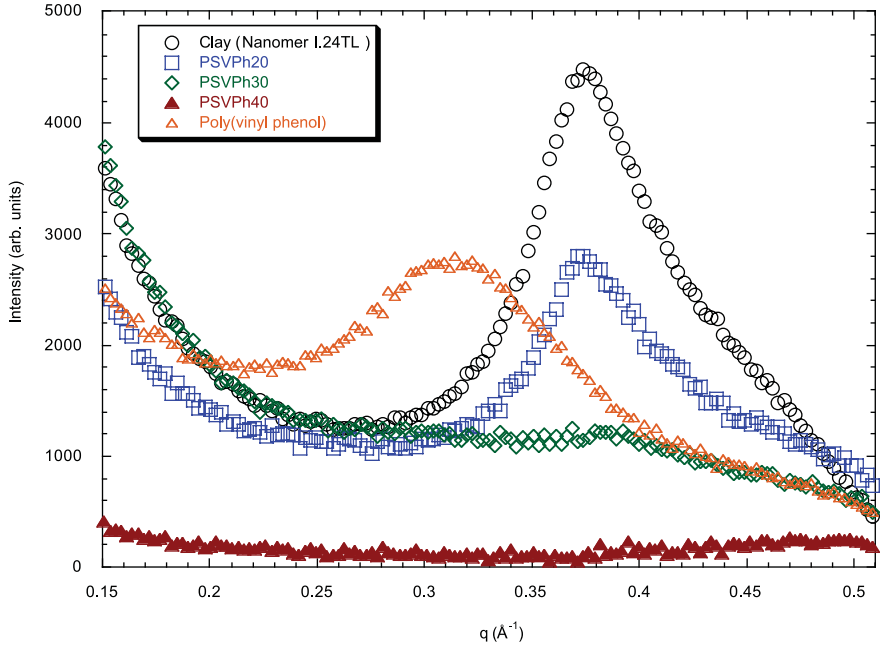

Fig. 6. Small angle X-ray patterns of nanocomposites containing 5 wt% Nanomer 1.24TL and various copolymers of styrene and vinyl phenol.

more detail in a forthcoming publication [36]. Moreover, similar results have been found for polymer nanotube nanocomposites [37].

While these results provide an indication of the importance of specific interactions between a polymer matrix and a nanoscale filler on the dispersion of polymer nanocomposites, they also provide specific guidelines to improve the dispersion and properties of nanocomposites. An optimum amount of intermolecular interactions between the polymer matrix and clay sheets provides a driving force for the polymer to exfoliate the layered silicate and individually disperse the sheets. Moreover, from a broader perspective, these results mimic those of the LCPU containing blends, in that the extent of intermolecular interactions between a polymer matrix and its filler can be optimized by spacing the –OH groups along the polymer chain, and this optimization provides a controllable mechanism to improve the dispersion of nanoscale fillers in a polymer matrix. Thus, careful control of the distribution of interacting groups along a polymer chain provides sufficient dynamic independence of the interacting moieties and allows the formation of the desired interparticle interactions. Our results indicate that this design concept appears to hold true for polymer blends and nanocomposites.

3.2. Improving polymer interfaces

As was demonstrated in Fig. 1, polymer–polymer interfaces are inherently weak due to the lack of entanglement between the two polymers. While the previous results provide a mechanism to vary the structure of one of the polymers to induce improved interaction between two polymers, it is not always feasible to allow this alteration, either chemically or economically. In these cases, there must be another method to improve the polymer interface. One possible method to improve the strength of the interface is to add a third polymer that can entangle with both polymers, stitch the two phases together and strengthen the overall polymer mixture, as is depicted in Fig. 7. In this scenario, the added polymer must 'like' both phases and thus an ideal candidate for this interfacial modifier is a copolymer of the two monomers that make up the homopolymers. In fact, this idea of a polymeric surfactant has been studied for many years [38–40], with diblock copolymers as one of the most studied interfacial modifiers. Unfortunately, diblock copolymers are not a commercially viable material as they are expensive and difficult to synthesize [41]. More importantly, the diblock copolymers tend to form micellar phases in these homopolymers rather than migrating to the polymer–polymer interface where they are needed.

However, there are a many different copolymers that can be synthesized from a mixture of A and B monomers. If only linear copolymers are considered, Fig. 8 shows a series of copolymers that can be synthesized from monomer A and

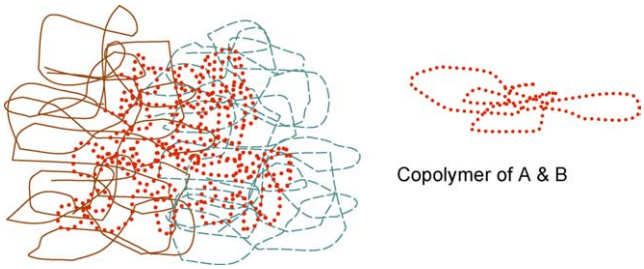

Fig. 7. Diagram of the strengthening of a polymer–polymer interface by a polymeric surfactant.

monomer B. At one end of this spectrum is the alternating copolymer, where every A monomer is surrounded by two B monomers, and every B monomer is surrounded by two A monomers. At the other end is a diblock copolymer where all the A monomers are surrounded by other A monomers, and every B monomer is surrounded by two B monomers, except at the one junction point in the middle. Half way in between these two limits is a statistically random copolymer where there is just as much probability that an A monomer is next to a B monomer as it is next to another A monomer. However, these are not the only options. A copolymer can be very blocky in nature, where there are long runs of A or B monomers, or the copolymer can have many AB dyads and, therefore, be very alternating in nature, but not truly an alternating copolymer. Moreover, this tendency to be alternating or blocky can be quantified by the parameter $P_x = P_{AB}/(P_A \times P_B)$, where P_{AB} is the percent of AB dyads along the chain and $P_{A(B)}$ is the percent of A(B) in the copolymer.

We recently presented the results of Monte Carlo simulation studies that examined which of the copolymers shown in Fig. 8 are most effective at compatibilizing polymer–polymer interfaces [42–44]. The interpretation of these results indicate that the 'random' copolymers that are more alternating in nature ($P_x \approx 1.5$) were poorest at strengthening interfaces, while the 'random' copolymers that were blocky ($P_x \approx 0.5$) provide the best improved strength at the interface. This conclusion developed from the observation that the blocky copolymers tend to expand at the interface the most and isotropically, indicating a conformation that is most likely to entangle with the homopolymer phases. This entanglement is envisioned to

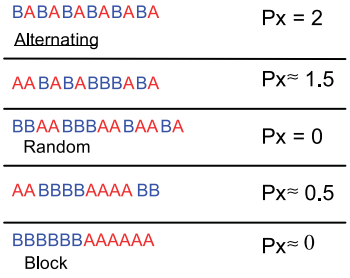

Fig. 8. Sequence distribution and its parameterization of linear copolymers comprised of monomer A and monomer B.

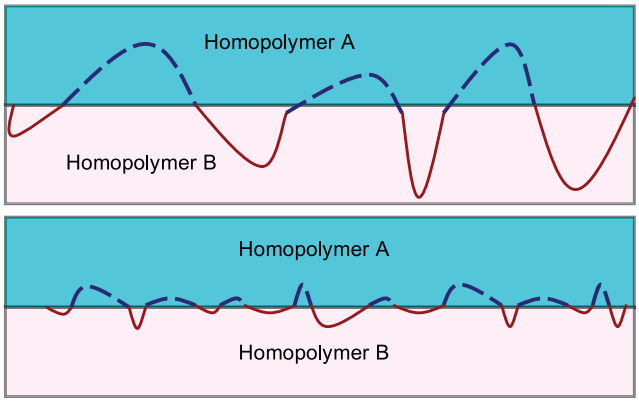

Fig. 9. Illustration of the importance of loops in a copolymer to effectively entangle with homopolymer phases.

occur at the homopolymer–homopolymer interface by the presence of long 'loops' that can expand into the homopolymer phases and entangle. This is illustrated diagrammatically in Fig. 9, which shows a blocky copolymer forming long loops into the homopolymer phases, which enables the formation of entanglements with the polymer matrix, while this mechanism is hindered in the more alternating copolymer structures.

While the results of this Monte Carlo study make sense, experimental verification of this trend was also desired. Thus, an experimental protocol was needed that provides a series of copolymers that ranged from alternating to diblock copolymers, as shown in Fig. 8, synthesized from the same monomer pair and a technique to monitor the strength of a polymer–polymer interface in the presence or absence of an interfacial modifier. These requirements were found with the monomer pair of styrene and methyl methacrylate, and the use of the asymmetric double cantilever beam technique to monitor the strength of the interface between poly(methyl methacrylate) and polystyrene that are modified with a range of copolymers.

Styrene and methyl methacrylate were chosen as the monomer pair in this study as various synthetic processes provide methods to obtain alternating [45], random, diblock and multiblock copolymers [6] of styrene and methyl methacrylate. Moreover, due to reactivity ratios, the random copolymer synthesized by traditional free radical techniques is slightly more alternating than random, and has a P_x value of 1.28. Thus, copolymers with P_x values of 2 (alternating), 1.28 ('random'), 0 (diblock), and multiblock copolymers that will have P_x values between 0 and 0.5 are possible to synthesize. It is also feasible to test their ability to strengthen the styrene–methyl methacrylate interface with the ADCB technique. This data will provide experimental evidence that can then be compared and contrasted to the Monte Carlo results presented above to examine the veracity of the predictions derived from the Monte Carlo work.

Thus the fracture toughness (G_c) of polystyrene–poly (methyl methacrylate) interfaces that are modified with the copolymers shown in Table 2 were determined using the asymmetric double cantilever beam technique. G_C for these modified interfaces as a function of the thickness of the copolymer film at the PS–PMMA interface is shown in Fig. 10. The data points at thicker copolymer layers describe the behavior of the interfaces that are saturated with the copolymer, and thus this portion of the plot most accurately quantifies the ability of the copolymers to strengthen the PS–PMMA interface. These results indicate that in terms of their ability to strengthen the copolymer interface:

pentablock > triblock > diblock > heptablock > random

These results are not exactly in agreement with the Monte Carlo results, but do provide further insight into the important parameters that control the ability of a copolymer to strengthen an interface. Monte Carlo simulation results suggest long runs of a given monomer along a copolymer chain (i.e. a blocky copolymer) will expand into the homopolymer phases, form loops that can entangle with the homopolymer, and strengthen the interface. A logical extension of this interpretation is that the more loops or blocks that exist in the copolymer, the stronger the interface will be. This interpretation leads to the prediction that the strength of the interfaces modified with the examined polymers should behave as:

Heptablock > pentablock > triblock > diblock > random

This prediction only differs from the experimental results with regard to the behavior of the heptablock copolymer. As we go from the pentablock to the triblock to the diblock copolymer, the number of times the copolymer crosses the interface decreases from 4 to 2 to 1, as illustrated in Fig. 11, and this logically corresponds to a decrease in the strength of the interface. However, as the number of blocks, increases to seven, the heptablock copolymer will cross

Table 2
Copolymers synthesized and examined as interfacial modifiers of polystyrene/poly(methyl methacrylate) interface

Block copolymer type	Block copolymer symbol	Block degree of polymerization	M_w	M_w/M_n
Diblock	S-M(100)	935-1050	201,500	1.19
Triblock (MMA centered)	S-M-S(50)	483-451-483	153,000	1.58
Triblock (Sty centered)	M-S-M(50)	485-481-485	170,000	1.53
Pentablock (MMA centered)	M-S-M-S-M(30)	298-296-290-296-298	159,000	1.51
Pentablock (Sty centered)	S-M-S-M-S(30)	301-305-276-305-301	175,000	1.52
Heptablock (MMA centered)	S-M-S-M-S-M-S(21)	197-219-218-213-218-219-197	151,000	1.54
Heptablock (Sty centered)	M-S-M-S-M-S-M(21)	200-216-201-199-201-216-200	155,000	1.58

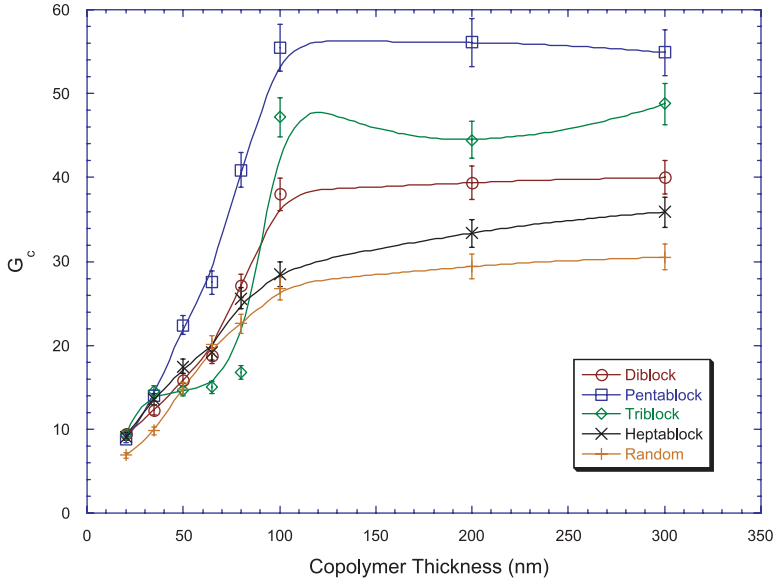

Fig. 10. Fracture toughness of PS/PMMA copolymers that are modified with various copolymers as a function of copolymer thickness at the interface.

the interface six times, and thus should be even stronger than the pentablock copolymer, however, this is not observed. Rather the strength of the interface modified by the heptablock copolymer approaches that of the interface that is modified with the random copolymer. This similarity between the heptablock and random copolymer can be rationalized by noting that the molecular weights of the multiblock copolymers are all similar ~150,000. Thus, as the copolymer becomes more blocky (i.e. contains more blocks), the length of each block must decrease. Thus, it appears that the block length of the heptablock is insufficient to efficiently entangle with the homopolymers, and thus does not strengthen the interface as effectively as the pentablock, triblock or diblock copolymers. Examination of Table 2 indicates that the diblock, triblock and pentablock copolymers have block lengths that are greater than ca. 30,000, while the heptablock has block lengths that average ca. 21,000. Thus, these results can be interpreted to indicate that there exists a critical block length for efficient entanglement between the multiblock copolymers and the homopolymer, which is evidently between 21,000 and 30,000 for the PMMA-PS system. It is interesting to note that this value is very similar to the entanglement molecular weights (M_e) of PS and PMMA, 31,000 and 27,500, respectively [46]. These results, therefore, document an additional parameter that was not previously recognized from the Monte Carlo results that is important in designing optimum polymeric interfacial modifiers, the block length. Both computational and experimental results demonstrate that multiblock or blocky copolymers are the optimal interfacial microstructure, however, the block length must also be sufficiently long to effectively entangle with the homopolymer.

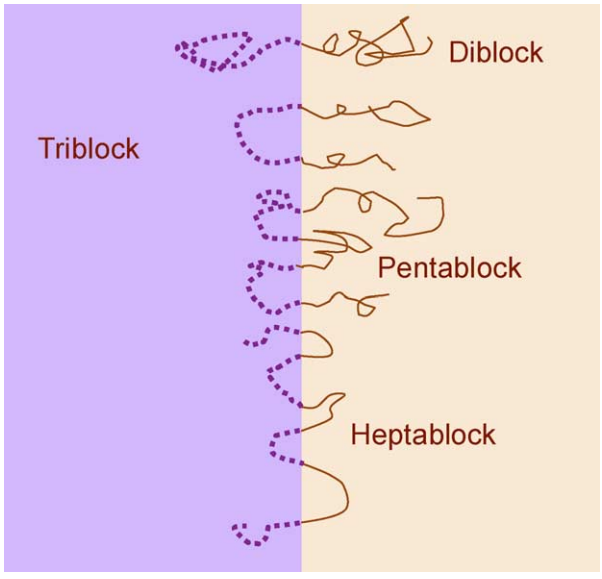

Fig. 11. Illustration of the ideal number of crossing of a given multiblock copolymer at a sharp polymer–polymer interface.

Thus, these results indicate that the formation of loops by long runs of a monomer within a copolymer chain is an efficient mechanism to strengthen a polymer–polymer interface. Moreover, this provides guidelines for other polymer interfacial modification procedures, suggesting that design of polymeric surfactants should concentrate on those structures that are blocky in nature and can provide a mechanism by which loops can entangle with a surrounding polymer matrix. Recent results from our group also document a reactive processing method that can be utilized to create these optimal 'blocky' copolymers, an in-situ processing technique using telechelic oligomers, which react to form the blocky compatibilizer at the interface via an interfacial condensation polymerization of the oligomers [47].

Table 3
Characteristics of Copolymers examined by neutron reflectivity

Abbreviated name	Copolymer description
Random	Random copolymer of styrene and methyl methacrylate
SMSMSMS-21	Heptablock copolymer with 21,000 molecular weight blocks
SMSMS-30	Pentablock copolymer with 30,000 molecular weight blocks
SMS-50	Triblock copolymer with 50,000 molecular weight blocks
Diblock	Diblock copolymer with 100,000 molecular weight blocks

3.2.1. Interphase structure determination

The analysis provided above is a logical interpretation of the data, especially in light of the previous computer simulation results. However, characterization of the modified polymer interphase provides a mechanism to further verify the proposed interpretation, i.e. that blocky copolymers are the optimum linear copolymer sequence distribution to strengthen polymer–polymer interfaces because they most effectively entangle with the homopolymer layers. If the blocky copolymers are indeed entangling with the homopolymers more effectively, this should manifest itself by forming broader interphases between the homopolymer and copolymer [48]. Thus, neutron reflectivity can be used to quantitatively determine the density profile of the PS–PMMA interfaces that have been modified with a random, a diblock, a triblock, a pentablock, and a heptablock copolymer to determine the actual structure of the copolymer/homopolymer interphases to test this interpretation. These experiments were completed at the NCNR at NIST and the properties of the polymers used in these experiments are shown in Table 3. The reflectivity samples were trilayers consisting of a 35 nm film of the copolymer sandwiched between 58 nm films of dPS and dPMMA on a silicon wafer. The sample was annealed for 12 h at 150 °C before their reflectivity curves were measured. The measured reflectivity curves were corrected and fit to obtain the scattering length density profile perpendicular to the wafer surface of the equilibrated trilayers to document the structure of the copolymer/homopolymer interphases. A representative reflectivity curve and fit is shown in Fig. 12 while the corresponding scattering length density profile is shown in Fig. 13.

The scattering length density profiles, such as the one in Fig. 13, is then analyzed to quantify the interfacial width between the *d*-polystyrene layer and the copolymer as well as the interfacial width between the *d*-PMMA and the copolymer by fitting the interfacial profile to a hyperbolic tangent,

$$Nb(z) = Nb_{\mathrm{ave}}[1 + \tan h(z/w_{\mathrm{I}})] \quad (3)$$

where w_{I} is the width of the interface. In this equation, $Nb(z)$ is the scattering length density of the sample at position z, Nb_{ave} is the scattering length density at the midpoint of the interface, and w_{I} is the interfacial width. Table 4 lists the copolymer thickness and the interfacial width of each copolymer–homopolymer interphase after annealing 12 h at 150 °C for the five samples studied. It can be seen from Table 4 that the layer of pentablock copolymer SMSMS-30 broadened from 350 to 520 Å upon annealing, an increase of 170 Å. Moreover, the width of the interphase between the copolymer and the dPS and dPMMA layers are 242 and 384 Å respectively. The thickness of the triblock copolymer SMS-50 layer also increased from 350 to 483 Å with a width of its interphase with dPS of 98 Å and a width of its interphase with dPMMA of

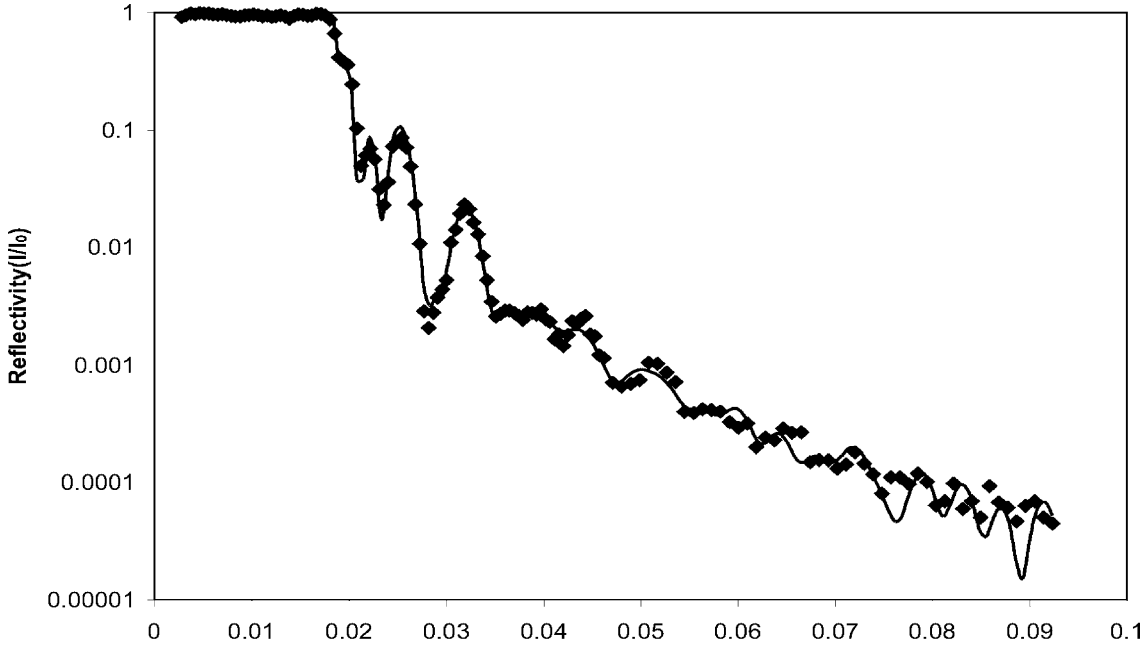

Fig. 12. Representative reflectivity curve and fit. This data set is for the random copolymer.

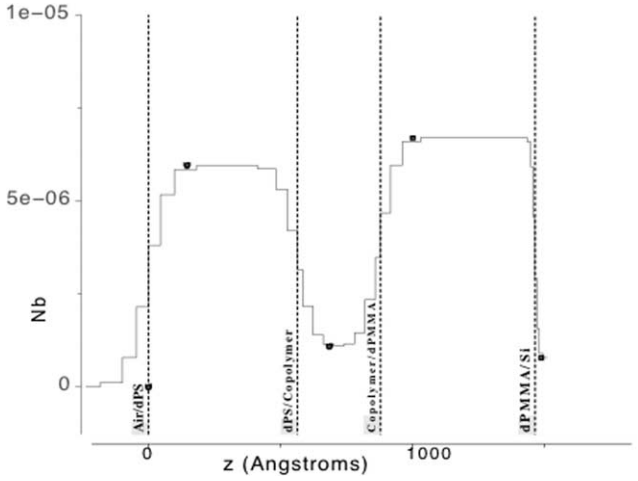

Fig. 13. Scattering length density profile of PS/PMMA interface that is modified by a random copolymer.

244 Å. The thickness of the three remaining copolymers did not significantly increase with annealing and exhibit minimal interfacial widths ($\leq$151 Å) with dPS and dPMMA.

The fracture toughness and interfacial widths of these interphases are also shown in Table 4. Two multiblock copolymers, SMSMS-30 and SMS-50, are clearly the best interfacial modifiers as quantified by the fracture toughness of the modified PS/PMMA interphase. The interphase that is modified with 300 nm of SMSMS-30 has a G_c of 60 J/m^2 and the interphase strengthened with SMS-50 has a G_c of 50 J/m^2. Both interphases have a fracture toughness that is at least 40% larger than the next strongest interphases. Thus, there appears to be a solid qualitative correlation between the interfacial thickness and fracture toughness of these modified interphases, where the broadest interphases exhibit the most strength.

However, to correlate this data to the formation of loops and entanglements, a molecular level picture must be invoked. A molecular level picture of this strengthening process undoubtedly involves entanglements of the copolymer with each homopolymer. The entanglements between the copolymer and homopolymer result in a broadening of the interphases that are monitored by neutron reflectivity. Conversely, an interphase where there exist fewer entanglements between the copolymer and homopolymer will have a smaller interfacial width. Thus, when the copolymer–homopolymer interphases are not symmetrical, the interphase with the smaller interfacial width (less entanglements) will likely be the source of mechanical failure. In this system, the smaller interfacial width is between the copolymer and dPS and is presumed to be the sight of failure. Thus in this study, the interphase between the dPS and copolymer will be the limiting structure in these modified dPS/dPMMA interphases and the one correlated to G_C.

In Table 4, it can be seen that the interfacial width of the interphases strengthened by the various copolymers corresponds well to their fracture toughness. The SMSMS-30

Table 4
Structural and mechanical properties of the polystyrene/copolymer/poly (methylmethacrylate) interfaces as determined by neutron reflectivity

Copolymer	Thickness (Å)	PS w_i (Å)	PMMA w_i (Å)	G_c (J/m^2)
Pentablock	520	242	384	22.4
Triblock	483	98	244	14.1
Diblock	331	149	151	15.9
Heptablock	328	141	144	16.8
Random	315	121	122	14.8

increased the fracture toughness of the interphase to 22 J/m^2 and the same copolymer layer grows to a thickness of 520 Å with a copolymer/dPS width of 242 Å. Both SMSMSMS-21 and the diblock copolymer exhibit an interfacial width with styrene of 141 and 149 Å respectively, and it follows that both polymers have the next highest fracture toughness in this series. The sequence is rounded out by the random copolymer with an interfacial width of 121 Å and a fracture toughness of 14.8 J/m^2 and SMS-50 with a fracture toughness of 14 J/m^2 and an interfacial width of 98 Å.

Previous studies have attempted to quantify the relationship between fracture toughness and interfacial width. Brown reported a model that relates the fracture toughness, G_c, to the energy required for craze fracture at a crack tip [49]. In this model, G_c is defined as:

$$G_c = G_c^*/\ln\{[1-(1.2\sigma_c/\sigma_f)^2]^{-1}\} \quad (4)$$

where G_c* is a constant and σ_c is the craze widening stress defined by

$$\sigma_c = f_{mono}\rho_{mer}w^*_{min}/2 \quad (5)$$

and σ_f is the fibril failure stress defined as

$$\sigma_f = f_{mono}\rho_{mer}w_{min}/2 \quad (6)$$

In both equations, f_{mono} is the static friction coefficient per monomer, ρ_{mer} is the number density of repeat units, and w_{min} is the width of the interphase where crazing is observed.

Substituting σ_f and σ_c in Eq. (4) yields the following relationship between the fracture toughness and interfacial width:

$$G_c = G_c^*/\ln\{[1-(1.2w^*_{min}/w_{min})^2]^{-1}\} \quad (7)$$

Additionally, Benkoski et al. [50] and, separately, Macosko [51] have found that the fracture toughness of a polymer interphase scales with the square of the interfacial width for a broad range of polymer structures, suggesting that this functionality has broad application to polymer–polymer interphases.

$$w^2_{(min)} \sim G_c \quad (8)$$

Thus, Fig. 14 shows a plot of the square of the interfacial width of the dPS/copolymer interphase as a function of its fracture toughness for our data. In this figure, the dotted line represents a linear fit to the data, which shows very good agreement with this theory.

Schnell and Creton have also studied the relationship between fracture toughness and the interfacial width [52,53]. These studies used polymers that were eight times larger than the entanglement molecular weight of the polymers and were homopolymer–homopolymer interphases. These experiments showed that the fracture toughness does not vary with interfacial width when the interfacial width is at least 12 nm. The data presented here differs from these results in that the fracture toughness of the interphase increases with interfacial width when the interfacial width is well above 12 nm. However, it should be noted that our data describe the ability of a copolymer to strengthen a homopolymer–homopolymer interphase, while Cretons work examined homopolymer–homopolymer interphases where the width was varied by altering the thermodynamic miscibility for the two polymers. For our compatibilizers studied, it was found that the fracture toughness increases with interfacial width up to (at least) 25 nm, suggesting that there exist fundamental differences between homopolymer–homopolymer interphases and those that are modified with a third component interfacial modifier. This may be explained as a continued increase in the number of entanglements between the copolymer and homopolymer as the interfacial width increases. These entanglements, therefore, may create stronger interphases than the homopolymer–homopolymer interphases studied by Schnell and Creton.

4. Conclusion

In this paper, two methods to improve the dispersion, interfacial adhesion and properties of polymer mixtures is presented. The data presented show that controlling the microstructure of the polymer components can optimize the amount of intermolecular hydrogen bonding between two polymers or between a polymer and nanofiller. More specifically, by spacing the hydrogen bonding groups on a copolymer chain, the amount of intermolecular hydrogen bonding is optimized. This correlation between interacting moiety spacing and extent of intermolecular interaction is attributed to the dynamic independence of the interacting functional groups. Moreover, the increased extent of intermolecular interactions is found to also correlate well to improved dispersions in polymer blends and polymer nanocomposites.

The second method provides an indication that multiblock or blocky linear copolymers are optimal at strengthening the biphasic interface between two polymers. By careful synthesis of a range of linear copolymer sequence distributions and subsequent examination of polymeric interfaces that are modified with these copolymers using ADCB and neutron reflectivity, the optimal sequence distribution is identified. These results provide guidelines by which novel and effective interfacial modifiers can be designed.

Acknowledgements

The authors would like to thank the National Science Foundation for financial support that funded this research through grants DMR-0241214 and CAREER-DMR-9702313 as well as a Collaborative Research in Chemistry Grant (CHE-0304807). They also acknowledge the support of the U.S.

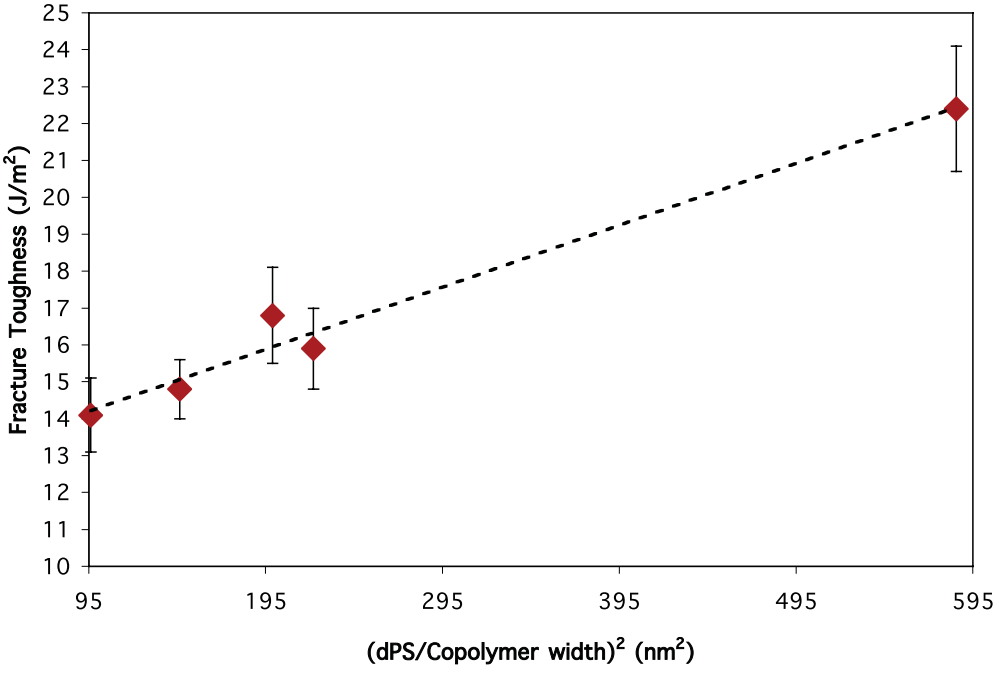

Fig. 14. Interfacial fracture toughness of compatibilized PS/PMMA interfaces as a function of the square of the interfacial width. The linearity of this plot agrees well with theory.

Department of Commerce National Institute of Standards and Technology, which provided the neutron research facilities used in this work and the University of Tennessee Neutron Sciences Consortium for financial support. Acknowledgement is also made to the Donors of the Petroleum Research Fund, administered by the American Chemical Society, for partial support of this research (PRF# 38740-AC7).

References

[1] Flory PJ. J Chem Phys 1942;10:51.
[2] Huggins ML. J Am Chem Soc 1942;64:1712.
[3] Flory PJ. Principles of polymer chemistry. Ithaca, New York: Cornell University Press; 1953.
[4] Paul DR, Bucknall CB. Polymer blends. New York: Wiley; 1999.
[5] Eastwood E, Dadmun MD. Macromolecules 2002;35:5069.
[6] Eastwood E, Dadmun MD. Macromolecules 2001;34:740.
[7] Viswanathan S, Dadmun MD. Macromol Rapid Commun 2001;22:779.
[8] Viswanathan S, Dadmun MD. Macromolecules 2002;35:5049.
[9] Khatri CA, Vaidya MM, Levon K, Jha SK, Green MM. Macromolecules 1995;28:4719.
[10] Char K, Brown HR, Deline VR. Macromolecules 1993;26:4164.
[11] Dadmun MD. Macromol Theory Simul 2001;10:795.
[12] Brown HR, Char K, Deline VR, Green PF. Macromolecules 1993;26:4155.
[13] Brown HR. Macromolecules 1989;22:2859.
[14] Brown HR. J Mater Sci 1990;25:2791.
[15] Sikka M, Pellegrini NN, Schmitt EA, Winey KI. Macromolecules 1997;30:445.
[16] Bernard B, Brown HR, Hawker CJ, Kellogg AJ, Russell TP. Macromolecules 1999;32:6254.
[17] Creton C, Kramer EJ, Hui C, Brown HR. Macromolecules 1992;25:3075.
[18] Kanninen MF. Int J Fract 1973;9:83.
[19] Hwang W-F, Wiff DR, Helminiak TE, Price G, Adams WW. Polym Eng Sci 1983;23:784.
[20] Hwang W-F, Wiff DR, Benner CL, Helminiak TE. J Macromol Sci, Phys 1983;B22:231.
[21] Pawlikowski GT, Dutta D, Weiss RA. Annu Rev Mater Sci 1991;21:159.
[22] Donald AM, Windle AH. Liquid crystalline polymers. Cambridge: Cambridge University Press; 1991.
[23] Flory PJ, Frost RS. Macromolecules 1978;11:1134.
[24] Flory PJ, Abe A. Macromolecules 1978;11:1119.
[25] Viswanathan S, Dadmun MD. Macromolecules 2003;36:3196.
[26] Viswanathan S, Dadmun MD. J Polym Sci, Polym Phys 2004;42:1010.
[27] Giannelis EP. Adv Mat 1996;8:29.
[28] Giannelis EP, Krishnamoorti R, Manias E. Adv Polym Sci 1999;138:107.
[29] Vaia RA, Giannelis EP. MRS Bull 2001;26:394.
[30] Reichert P, Nitz H, Klinke S, Brandsch R, Thomann R, Mülhaupt R. Macromol Mater Eng 2000;275:8.
[31] Hasegawa N, Okamoto H, Kawasumi M, Kato M, Tsukigase A, Usuki A. Macromol Mater Eng 2000;280–281:76.
[32] Kawasumi M, Hasegawa N, Kato M, Usuki A, Okada A. Macromolecules 1992;30:6333.
[33] Hasegawa N, Kawasumi M, Kato M, Usuki A, Okada A. J Appl Polym Sci 1998;67:87.
[34] Kato M, Usuki A, Okada A. J Appl Polym Sci 1997;66:1781.
[35] Usuki A, Kato M, Okada A, Kurauchi T. J Appl Polym Sci 1997;63:137.
[36] Kumar D, Dadmun MD. in preparation.
[37] Rasheed A, Britt PF, Dadmun MD. in preparation.
[38] Fayt R, Jérôme R, Teyssié Ph. J Polym Sci, Polym Lett Ed 1981;19:79.
[39] Fayt R, Jérôme R, Teyssié Ph. J Polym Sci, Polym Phys Ed 1981;19:1269.
[40] Fayt R, Jérôme R, Teyssié Ph. J Polym Sci, Polym Phys Ed 1982;20:2209.
[41] Hamley IW. The physics of block copolymers. Oxford: Oxford University Press; 1998.
[42] Dadmun MD. Macromolecules 1996;29:3868.
[43] Dadmun MD. Macromolecules 2000;33:9122.
[44] Dadmun MD. Macromol Theory Simul 2001;10:795.
[45] Galvin ME. Macromolecules 1991;24:6354.
[46] Fried JR. Polymer science and technology. Upper Saddle River, NJ: Prentice Hall; 1995.
[47] O'Brien C, Rice JK, Dadmun MD. Eur Polym J 2004;40:115.
[48] Helfand E, Tagami Y. J Chem Phys 1972;56:3592.
[49] Brown HR. Macromolecules 2001;34:3720.
[50] Benkoski J, Fredrickson GE, Kramer EJ. J Polym Sci, Part B: Polym Phys 2001;39:2363.
[51] Cole PJ, Cook RF, Macosko CW. Macromolecules 2003;36:2808.
[52] Schnell R, Stamm M, Creton C. Macromolecules 1999;32:3420.
[53] Creton C. Contact Angle Wettability Adhes 2002;2:1.

Mark D. Dadmun's current research interests seek to understand how the propeties of multi-component polymer systems, such as blends, nanocomposites, multi-layers, or composites, can be optimized through microscopic manipulations. Specific projects include improving the dispersion of polymer blends and nanocomposites by optimizing specific interactions between components, developing methods to modify and control polymer interfaces and surfaces including formation of molecular loops, and optimizing the surface segregation process of surface-active additives in bulk polymers. The modification of interfaces with polymers to design new materials with targeted surface-sensitive properties is of particular interest.

He received his Ph.D. from the University of Massachusetts in Polymer Science and Engineering in 1991, and was awarded a National Research Council Post-doctoral fellowship, which he completed at the National Institute of Standards and Technology. He joined the faculty of the Chemistry Department at the University of Tennessee in 1994, where he was recently promoted to Full Professor. He was also appointed as a Joint Faculty member at Oak Ridge National Laboratory in 2005.

Mark Dadmun was also awarded *National Science Foundation CAREER Award* in 1997 for his work on blending liquid crystalline polymers with amorphous polymers. He serves on the Editorial Advisory Board of *European Polymer Journal* and has coauthored over 50 articles and books.